PROCEEDINGS OF SCIENCE

# Rho-rho production in two-photon collisions

**Klaus Freudenreich**[∗†]
*Labor für Hochenergiephysik, ETH Zürich, Switzerland*
*E-mail:* Klaus.Freudenreich@cern.ch

The measurement of exclusive $\rho\rho$ production in two-photon interactions at LEP, $\gamma\gamma^* \to \rho\rho$, was studied at two-photon center-of-mass energies of 1.1 GeV $\leq W_{\gamma\gamma} \leq$ 3 GeV and photon virtualities of $Q^2 < 0.02$ GeV$^2$ and $0.2 \leq Q^2 \leq 30$ GeV$^2$. These data allow on the one hand a comparison to QCD and the generalised vector dominance model (GVDM). On the other hand, the large kinematical range permits to check models with exotic mesons.

*International Europhysics Conference on High Energy Physics*
*July 21st - 27th 2005*
*Lisboa, Portugal*

∗Speaker.
†On behalf of the L3 collaboration.

 

PoS(HEP2005)112

## 1. Introduction

The two-photon process
$$e^+e^- \rightarrow e^+e^-\gamma\gamma^* \rightarrow e^+e^-\rho\rho \quad (1.1)$$
has already been measured at lower $e^+e^-$ c.m. energies [1] but mostly without tagging. The data presented here were obtained with tagging, thus allowing to cover a larger range in the virtuality of one of the interacting photons, i.e. $0.2 \leq Q^2 \leq 30$ GeV$^2$. For comparison, also preliminary untagged data at $Q^2 < 0.02$ GeV$^2$ will be shown. Both $\rho^0\rho^0 \rightarrow \pi^+\pi^-\pi^+\pi^-$ and $\rho^+\rho^- \rightarrow \pi^+\pi^0\pi^-\pi^0$ channels are studied. The large range in the two-photon c.m. energy, 1.1 GeV $\leq W_{\gamma\gamma} \leq$ 3 GeV allows to study resonance production in t-channel exchange as well as to search for exotic mesons.

## 2. Data

The data were taken with the L3 detector [2] at LEP (Fig. 1).

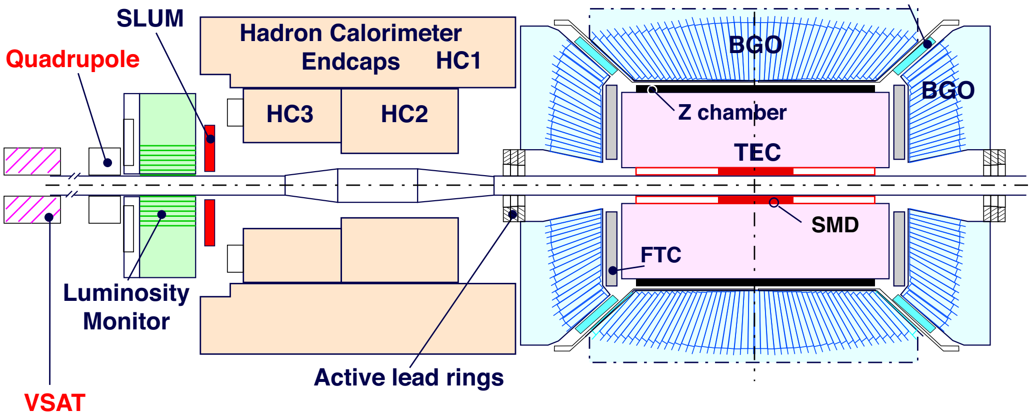


**Figure 1:** Sketch (sideview) of the L3 detectors used in this analysis.

The L3 detector was well suited for this search because there was only a small amount of material in front of the electromagnetic BGO calorimeter (0.2 of a radiation length). This yielded a low threshold in photon energies ($\geq$ 60 MeV) and in momentum measurements of charged tracks ($p_T \geq$ 100 MeV). Two detectors were used for tagging: a) The so called very small angle tagger (VSAT) detectors, situated on either side of the interaction point (IP) at a distance of 8.17 m, behind the first quadrupole. It consisted of 4 BGO crystal calorimeters. b) The luminosity monitors situated at either side of the IP at a distance of 2.73 m, each consisting of 2 detectors with 304 BGO crystals per detector.

In the following, the data will be divided into four intervals in $Q^2$:

1. $Q^2 < 0.02$ GeV$^2$, no electron tag, $Q^2$ calculation from the 4 $\pi$ state,
2. 0.2 GeV$^2 < Q^2 < 0.85$ GeV$^2$, electron tag from the VSAT, $Q^2$ calculation from the $4\pi$ state,
3. 1.2 GeV$^2 < Q^2 < 8.5$ GeV$^2$ electron tag and $Q^2$ calculation from the luminosity monitor,
4. 8.8 GeV$^2 < Q^2 < 30$ GeV$^2$, electron tag and $Q^2$ calculation from the luminosity monitor.

The tagged data were taken at 91 GeV $\leq \sqrt{s} \leq$ 209 GeV with an integrated luminosity of 854.7 pb$^{-1}$ [3]. The untagged data were taken at 161 GeV $\leq \sqrt{s} \leq$ 209 GeV with an integrated luminosity of 697.7 pb$^{-1}$ [4].

Fig. 2 shows the four-pion mass distribution (W$_{\gamma\gamma}$) and the 4 possible mass combinations M($\pi^{\pm}\pi^{0}$) (within 1.1 GeV $\leq W_{\gamma\gamma} \leq$ 3 GeV) for the reaction $e^+e^- \to e^+e^-_{tag}\pi^+\pi^-\pi^0\pi^0$ for 0.2 GeV$^2$ < Q$^2$ < 0.85 GeV$^2$. A clear $\rho^{\pm}$ signal is observed in M($\pi^{\pm}\pi^{0}$).

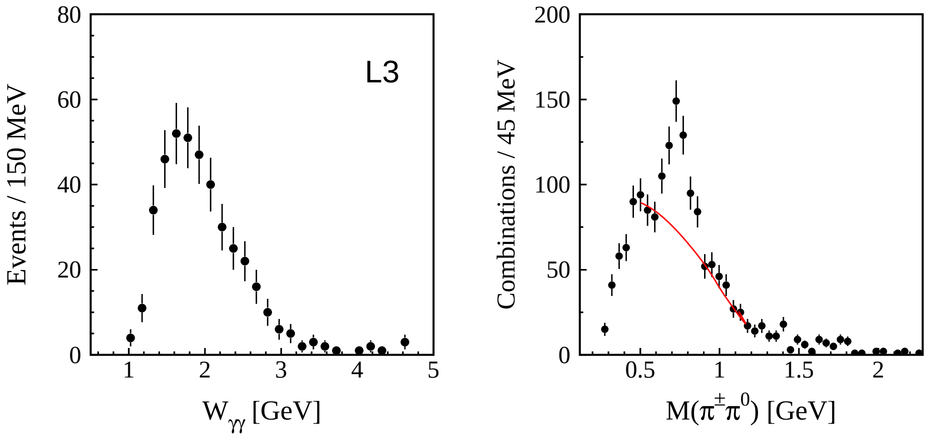


**Figure 2:** M($\pi^+\pi^-\pi^0\pi^0$) (left) and M($\pi^{\pm}\pi^{0}$), 4 entries per event (right).

Fig. 3 shows the 4 pion invariant mass distribution (W$_{\gamma\gamma}$) and the 4 possible mass combinations M($\pi^+\pi^-$) (within 1.1 GeV $\leq W_{\gamma\gamma} \leq$ 3 GeV) for the reaction $e^+e^- \to e^+e^-_{tag}\pi^+\pi^-\pi^+\pi^-$ for 0.2 GeV$^2$ < Q$^2$ < 0.85 GeV$^2$. A strong $\rho^0$ signal is observed in M($\pi^+\pi^-$).

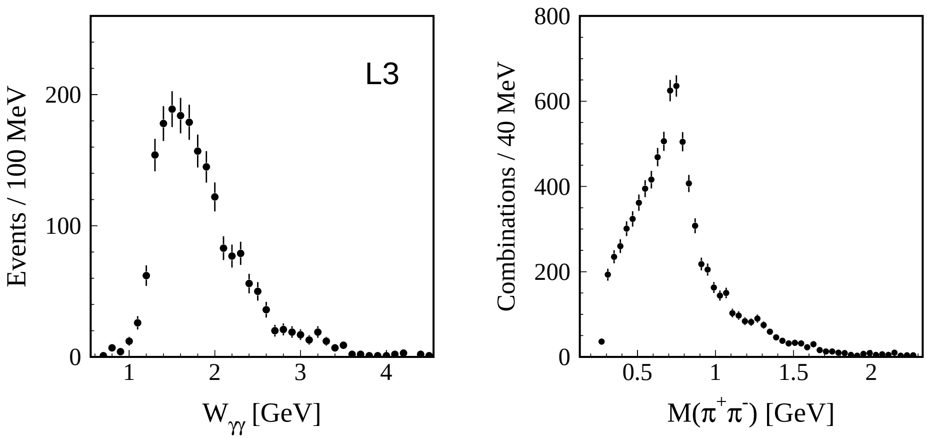


**Figure 3:** M($\pi^+\pi^-\pi^+\pi^-$) (left) and M($\pi^+\pi^-$), 4 entries per event (right).

The fraction of $\rho\rho$ events was determined by a maximum likelihood fit in intervals of Q$^2$ and W$_{\gamma\gamma}$. For the background, the following processes were considered: $\gamma\gamma^* \to \rho\pi\pi$, $\gamma\gamma^* \to a_2^{\pm}(1320)\pi^{\mp}$, $\gamma\gamma^* \to f_2\pi\pi$ and nonresonant $\gamma\gamma^* \to \pi\pi\pi\pi$.

The cross section $\sigma_{\gamma\gamma}(\gamma\gamma^* \to \rho\rho)$ was obtained from the the $\sigma_{ee}(e^+e^- \to e^+e^-\rho\rho)$ cross section via $\sigma_{ee} = L_{TT} \cdot \sigma_{\gamma\gamma}$ where $L_{TT}$ is the two-photon luminosity function which is calculated using the program GALUGA [5].

## 3. Results

Fig. 4 shows the $\gamma\gamma \to \rho^0\rho^0$ and $\gamma\gamma \to \rho^+\rho^-$ cross sections as a function of the four-pion masses in the four $Q^2$ intervals mentioned above.

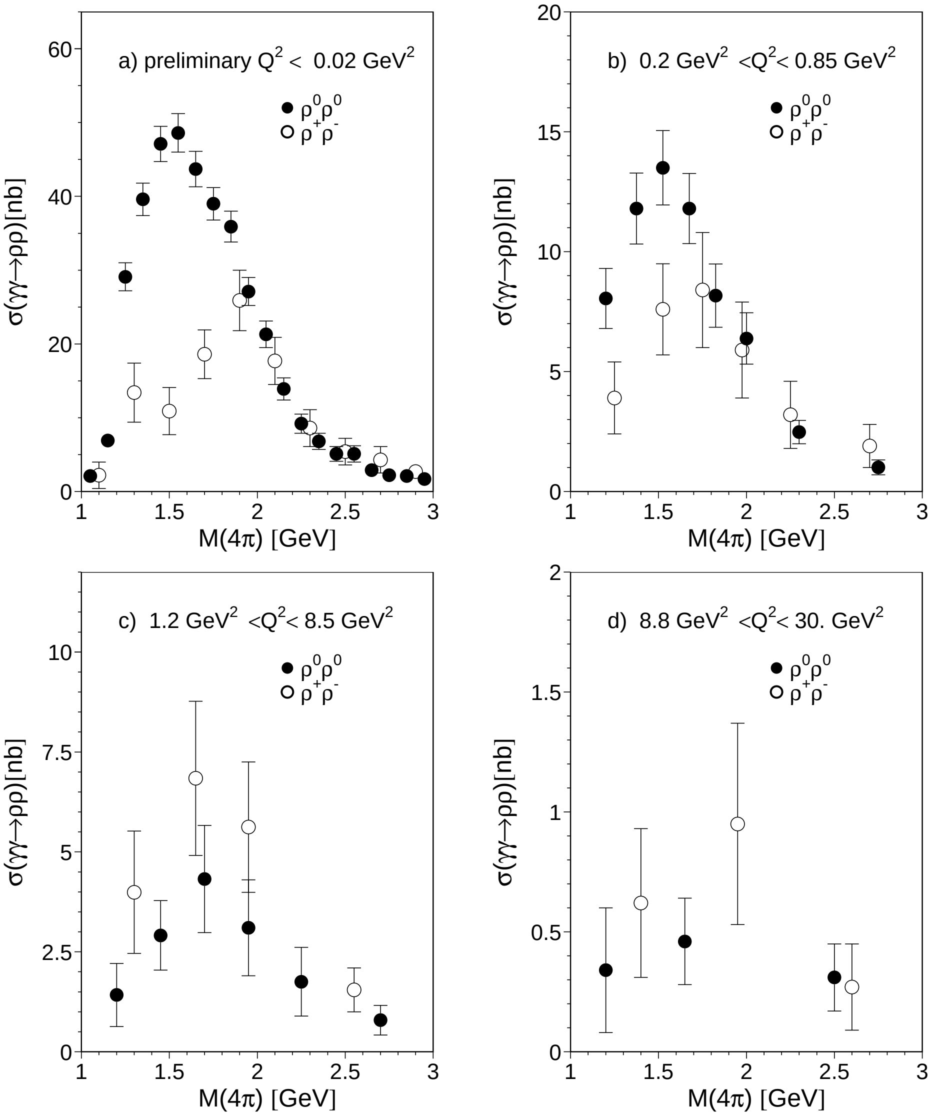


**Figure 4:** The $\gamma\gamma \to \rho^0\rho^0$ and $\gamma\gamma \to \rho^+\rho^-$ cross sections as a function of the four-pion mass a) at $Q^2 \leq 0.02 GeV^2$, b) $0.20 GeV^2 \leq Q^2 \leq 0.85 GeV^2$, c) $1.2 GeV^2 \leq Q^2 \leq 8.5 GeV^2$ and d) $8.8 GeV^2 \leq Q^2 \leq 30 GeV^2$.

For an isospin I = 0 state the ratio R of $\sigma(\gamma\gamma \to \rho^+\rho^-)/\sigma(\gamma\gamma \to \rho^0\rho^0)$ is equal two. We observe this for $Q^2 > 1.2\ GeV^2$. At low $Q^2$, however, this ratio is reversed to R = 0.42 $\pm$ 0.05 $\pm$ 0.09 for $Q^2 < 0.02\ GeV^2$. This strong enhancement of $\rho^0\rho^0$ with respect to $\rho^+\rho^-$ at the lowest $Q^2$ value was interpreted as evidence for an isospin 2 resonance [6].

In Fig. 5 the cross section $d\sigma_{ee}/dQ^2$ is compared to a QCD-based calculation [7] and the $\sigma_{\gamma\gamma}$ cross section is compared to a parametrisation based on the GVDM model [8]. The QCD parametrisation fits both $\sigma(\rho^+\rho^-)$ and $\sigma(\rho^0\rho^0)$ well over four orders of magnitude. There is a crossover of the cross sections at a $Q^2$ of around 1 GeV$^2$ suggesting a different production mechanism at low and high $Q^2$. The GVDM parametrisation reproduces only $\sigma(\rho^0\rho^0)$ well. The $Q^2$ evolution of $\sigma(\rho^+\rho^-)$ cannot be described by this parametrisation. A $\rho$-pole fit to the data fails for both the $\rho^0\rho^0$ and the $\rho^+\rho^-$ cross sections.

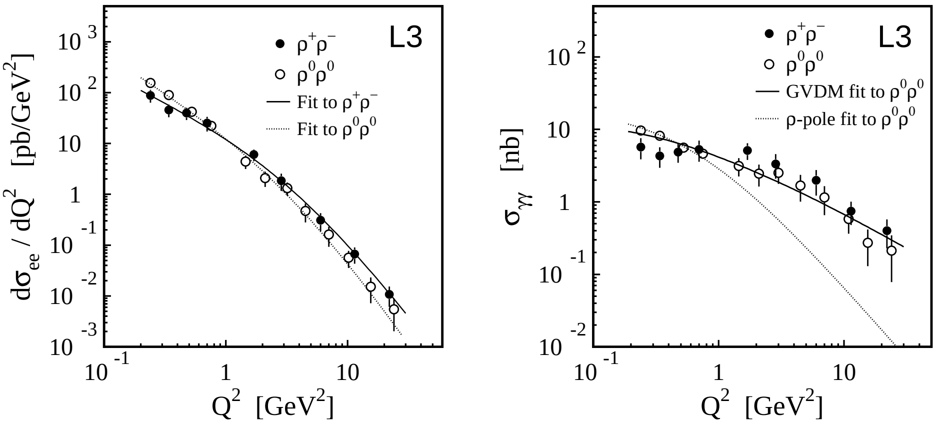


**Figure 5:** $\frac{d\sigma_{ee}}{dQ^2}$ (left) and $\sigma_{\gamma\gamma}$ (right) as a function of $Q^2$.

## 4. Acknowledgements

I would like to thank my colleagues from the L3 Two-Photon group for their advice: J. Field, M. Kienzle, G. Sultanov and I. Vorobiev.

## References

[1] M. Althoff et al., *Z. Phys.* **C 16** (1982) 13; Ch. Berger et al., *Z. Phys.* **C 38** (1988) 521; W. Braunschweig et al., *Z. Phys.* **C 41** (1988) 353; H. Albrecht et al., *Z. Phys.* **C 50** (1991) 1; H. Albrecht et al., *Phys. Lett.* **B 267** (1991) 535.

[2] B. Adeva et al., Nucl. Instr. and Methods **A 289** (1990) 35; M. Chemarin et al., Nucl. Instr. and Methods **A 349** (1994) 345; M. Acciarri et al., Nucl. Instr. and Methods **A 351** (1994) 300; I.C. Brock et al., Nucl. Instr. and Methods **A 381** (1996) 236; A. Adam et al., Nucl. Instr. and Methods **A 383** (1996) 342.

[3] P. Achard et al., *Phys. Lett.* **B 568** (2003) 11, P. Achard et al., *Phys. Lett.* **B 597** (2004) 26, P. Achard et al., *Phys. Lett.* **B 604** (2003) 48, P. Achard et al., *Phys. Lett.* **B 615** (2005) 19.

[4] L3 Coll., in preparation.

[5] G.A. Schuler, *Comp. Science Commun.* **108** (1998) 279.

[6] I.V. Anikin, B. Pire and O.V. Teryaev, *Phys. Lett.* **B 626** (2005) 86.

[7] M. Diehl, T. Gousset and B. Piere, *Phys. Rev.* **D 62** (2000) 073014.

[8] J.J. Sakurai and D. Schildknecht, *Phys. Lett.* **B 40** (1972) 121; I.F. Ginzburg and V.G. Serbo, *Phys. Lett.* **B 109** (1982) 231.